N_2O Laser Absorption Measurements During Toluene/N_2O Combustion

Olivier Mathieu[1], Atmadeep Bhattacharya[2], Claire M. Grégoire[1], Eric L Petersen[1]
[1]J. Mike Walker '66 Department of Mechanical Engineering, Texas A&M University
College Station, TX, USA
[2]Department of Mechanical Engineering, Aalto University School of Engineering
Otakaari 4, Espoo, 02150, Finland

1 Introduction

Using ammonia as a fuel is emerging as a possible solution to produce energy while mitigating carbon emissions and the associated global warming [1]. However, ammonia suffers from many drawbacks when used as a fuel; including a very slow flame speed and narrow flammability limits [2], and high ignition temperatures [3] compared to traditional hydrocarbon-based fuels. To lessen these issues, it is often considered to burn ammonia in a dual-fuel configuration. For instance, in internal combustion engines, several studies have considered ammonia/gasoline blends to power spark-ignition engines in passenger cars (see [4] and references therein).

In an internal combustion engine, due to the presence of residual gases from the previous combustion cycle, it is important to understand the interactions between the fresh charge and the combustion products from the previous cycles, which also include pollutants and unburned species. Notably, N_2O is an important combustion intermediate of ammonia combustion [5], for which emissions must be strictly limited due to its very high global warming potential of about 300 times that of carbon dioxide on a 100-year timescale. Furthermore, N_2O emissions are expected to remain the dominant ozone-depleting substance in the stratosphere throughout the 21st century [6].

Toluene is present in gasoline and is also generally considered as representative of the aromatic class of hydrocarbons present in gasoline. Studying the interactions between toluene and N_2O is therefore necessary for the efficient co-combustion of ammonia and gasoline in spark-ignition engines, especially because the literature is very limited for that system [7,8]. To address this gap, the aim of this study is to provide fundamental data for model validation. Specifically, the decomposition of N_2O was followed behind reflected shock waves using a laser absorption diagnostic during the oxidation of toluene by N_2O in highly dilutes mixtures. The results were compared to predictions from detailed kinetics models from the literature. To the best of our knowledge, there are only two groups producing models describing the oxidation of toluene with a detailed NOx sub-mechanism: Curran's group at NUI Galway [9] and the CRECK group at POLIMI [10]. Note that Liang et al., 2024 also propose a model describing the interactions between gasoline and N_2O [11], but the hydrocarbon sub-mechanism is based on an earlier version of Curran group one and was thus not used herein.

Correspondence to: olivier.mathieu@tamu.edu

2 Experimental setups

2.1. Shock Tube and Conditions Investigated

Experiments were conducted in the Aerospace Shock Tube (AST) at Texas A&M University. This facility is made of stainless-steel and set up for chemical kinetics measurements at low-to-intermediate pressure conditions using laser absorption experiments. The driver section has a 7.62-cm inner diameter and is 3.25 m long, while the driven section has a 16.2-cm inner diameter and is 7.88 m long. These two parts are separated by a single polycarbonate diaphragm and a cross-shaped cutting blade is used to facilitate the diaphragm's rupture and initiate shock propagation.

To measure the incident-shock velocity, five piezoelectric pressure transducers (PCB P113A) were employed to detect non-intrusively the shock passage over the last 2 m of the shock tube. The temperature (T_5) and pressure (P_5) behind the reflected shock wave were calculated using a code based on the 1-D normal shock equations within uncertainties of ±1% and ±0.8%, respectively. The shock tube has a vacuum system utilizing a rotary vane pump (Agilent DS 402) and a turbomolecular pump (Agilent Turbo V1001 Navigator) to achieve pressures of 10^{-8} atm or less prior to each test. Gas pressures are measured using capacitance manometers (MKS Baratrons with 0 – 10 and 0 – 1000 Torr ranges). Optical windows ports are located at the same axial plane near the endwall to enable laser absorption measurements. Finally, three mixtures of toluene (C_7H_8) and nitrous oxide (N_2O) were studied in 0.2/0.79 He/Ar (He is typically added to expedite the vibrational relaxation, see [12] for more details) at three equivalence ratios (ϕ = 0.5, 1.0, and 2.0) for temperatures (T_5) and pressures (P_5) ranging from 1511 to 1868 K and from 1.20 to 1.32 atm, respectively. Table 1 provides the species mole fractions of the mixtures and summarizes the experimental conditions covered during the course of this study. Lastly, the liquid C_7H_8 comes from Sigma Aldrich with a purity of 99.8%, and all the gases were provided by Linde: N_2O with a purity ≥ 99%, He and Ar with 99.999% purity.

Table 1: Mixture composition and experimental conditions for C_7H_8/N_2O mixtures in 0.2/0.79 He/Ar.

ϕ	X_{C7H8}	X_{N2O}	Temperature (K)	Pressure (atm)
0.5	0.00027	0.00973	1511 - 1820	1.21 – 1.30
1.0	0.000526	0.009474	1599 – 1868	1.20 – 1.32
2.0	0.001	0.009	1577 – 1804	1.20 – 1.29

2.2. N_2O Laser Diagnostic

A tunable quantum cascade laser (QCL), initially designed for CO absorption measurements, was tuned to monitor the N_2O decomposition behind reflected shock waves during the oxidation of toluene (C_7H_8) by N_2O. With a range of 2056 – 2064 cm^{-1}, the tunable QCL can access the P(128e) transition line of N_2O in the fundamental band (1 ← 0) at 2062.026 cm^{-1}. The calculations of the fractional absorbance, carried out using the HITEMP database [13] for N_2O in the tunable range, show a fairly good 15% absorbance with the following parameters: X_{N2O} = 9,000 ppm, 1700 K, 1.3 atm, and a path length of 16.2 cm (shock-tube I.D.). Note that the laser absorption diagnostic is working in good isolation from the CO transition line, as well as common combustion intermediate products, such as H_2O and CO_2, to cite a few. The laser beam was divided into two distinct paths: the incident intensity I_0 and the transmitted intensity I_t passing through the reacting gases in the shock tube. Both are collected separately by two InSb detectors after passing a direct-absorption setup consisting of lenses and bypass filters (Thorlabs). The wavelength was centered and verified before each test with a flip mirror sending the light into a wavemeter (Bristol 671). Finally, the time-resolved N_2O mole fractions are calculated with these two intensities (I_0 and I_t) using the Beer-Lambert relation, defined as $I_t/I_0 =$

$exp(-k_\nu PLX_{N2O})$, where k_ν is the absorption coefficient, P is the pressure, L is the path length (shock-tube I.D.), and X_{N2O} is the N_2O mole fraction. The absorption coefficient was calibrated for a large range of temperatures and pressures, namely 710 – 1392 K near 0.205 – 0.406 atm using T_2, P_2 (Low temperature, LT) and 1225 – 1904 K near 1.13 – 1.59 atm using T_5, P_5 (High temperature, HT) as can be seen in Fig. 1. For the current experiments, the calibration using T_5 and P_5 is needed and is described using Eqn. 1 and 2 for the highest temperatures (1700 – 1900 K).

$$k_{\nu,LT} = 5.273 \times 10^{15} \times T^{-4.8961} \quad (1)$$

$$k_{\nu,HT} = 5.964 \times 10^{6} \times T^{-2.0201} \quad (2)$$

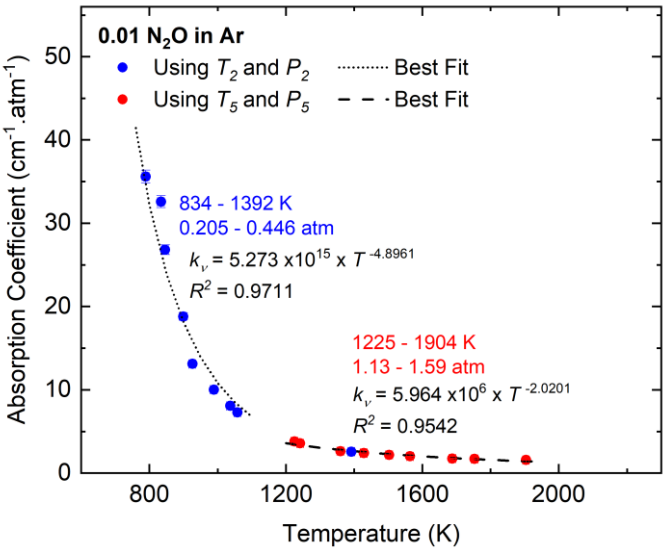

Figure 1: Characterization of the temperature dependence of the absorption coefficient for 0.01 N_2O in Ar using the P(128e) transition line of N_2O in the fundamental band (1 ← 0) at 2062.026 cm^{-1}. Data were taken at T_2, P_2 (710 - 1392 K, 0.205 - 0.446 atm), and T_5, P_5 (1225 - 1904 K, 1.13 - 1.59 atm).

A mixture of N_2O in 0.99 Ar was studied behind reflected shock waves to obtain the calibration results and characterize the absorption capability of the P(128e) transition line of N_2O in a bath of Ar. An uncertainty analysis, where the root sum square method was done, consisted in perturbing several factors that are part of the k_ν calculations and noting the change that echoes in the final k_ν. Three parameters are considered in this study: P ($\pm$1%), L ($\pm$0.1 cm), and X_{N2O} ($\pm$3%, based on [22]) that induce a difference of 1%, 0.6%, and 3%, respectively, leading to a 4.6% total uncertainty on k_ν, and on the N_2O mole fraction. During the experiments, the exothermicity from the reaction of C_7H_8 with N_2O induces an increase in the temperature T_5 during the process. These changes in temperature were accounted for using Eqns. 1 and 2, creating an adapted time-varying absorption coefficient with the temperature variation predicted by the current model presented herein. The high dilution was chosen to keep the temperature change below 150 K (ΔT = 80 – 120 K), minimizing any uncertainties from the temperature predictions of the model.

3 Experimental Results and Model Comparison

The N_2O profiles obtained during this study are visible in Fig. 2 for (a) ϕ = 0.5, (b) ϕ = 1.0, and (c) ϕ = 2.0. For the fuel-lean case, no apparent consumption of N_2O is observed for the coldest temperature investigated, 1511 K, within the time frame of the experiment. Above this temperature, the N_2O mole fraction starts decreasing right from the beginning of the experiment. Increasing the temperature leads to a faster consumption of N_2O, although it is worth mentioning that the N_2O mole fraction never reaches

zero in our conditions. For the stoichiometric and fuel-rich mixtures, similar observations can be made except that the mole fraction reaches zero for these mixtures. Moreover, for the coldest temperatures investigated with the stoichiometric mixtures, a rapid change in the rate of N_2O consumption can be observed at around 1500 µs and 2000 µs for the 1619 K and 1599 K cases, respectively, indicating a possible change in the consumption pathway. Note that comparing the three equivalence ratios at similar temperatures (1690 K, 1694 K, and 1707 K, and 1596 K, 1599 K, and 1581 K for ϕ = 0.5, 1.0, and 2.0, respectively) does not show major differences between the profiles, except the aforementioned change in the consumption rate at 1599 K, ϕ = 1.0. This indicates that the N_2O consumption is relatively independent of the equivalence ratio in our conditions. These results and observations will be discussed using the NUIG model in the next section.

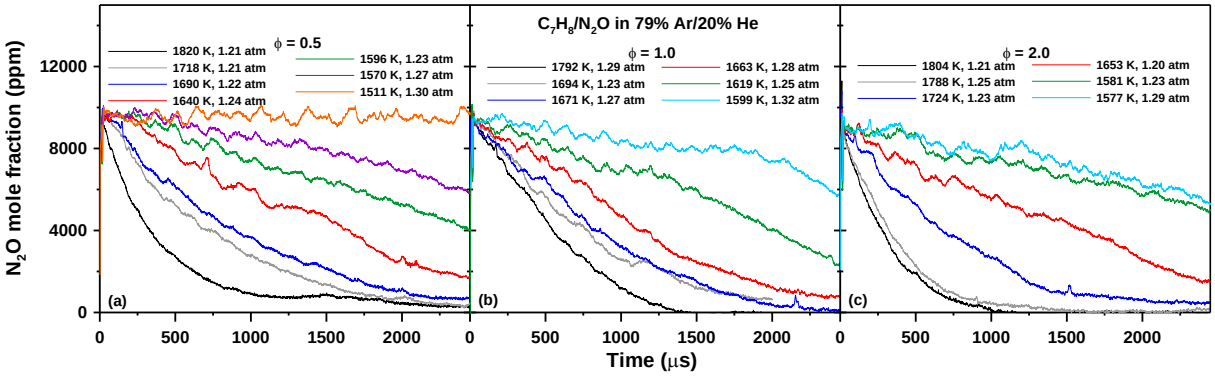

Figure 2: Evolution with time of the N_2O mole fraction during the oxidation of toluene by N_2O for mixtures diluted in 99% Ar and He. (a) ϕ = 0.5, (b) ϕ = 1.0, and (c) ϕ = 2.0.

4 Model Comparison and Discussion

Selected N_2O profiles on the low- and high-temperature extremes of the ranges investigated were compared to the model predictions in Fig. 3. Overall, the fuel-lean mixture is well predicted by the models, notably by the NUIG model at low temperature. On the other hand, both models predict a full consumption of N_2O at high temperature, which is not observed experimentally. For the stoichiometric case, both models tend to be over-reactive over the entire range of temperatures investigated, with the NUIG model being the closest to the data. Note that the change of slope in the N_2O consumption observed experimentally is also seen for the models, although the change is not as abrupt as for the experiment. Lastly, for the fuel-rich case, the models are still relatively close to the data but they tend to be under-reactive, especially for the NUIG model.

A numerical analysis based on rate of production and reaction pathway analyses was conducted using the NUIG model to understand better the results. Under our conditions, the reactivity is actually initiated by the thermal decomposition of toluene, forming the radical H and the benzyl radical ($C_6H_5CH_2$). This H radical will then attack the N_2O to form OH via $N_2O + H \leftrightarrows N_2 + OH$, with also a strong contribution from the thermal N_2O decomposition via (N_2O (+M) $\leftrightarrows N_2 + O$ (+M) with regards to N_2O consumption. Note that all these radicals H, OH, and O also then attack toluene and its combustion intermediates. The fact that N_2O consumption essentially only depends on the initial decomposition of toluene and on the thermal dissociation of N_2O explains why the N_2O profiles are relatively insensitive to the equivalence ratio under our conditions.

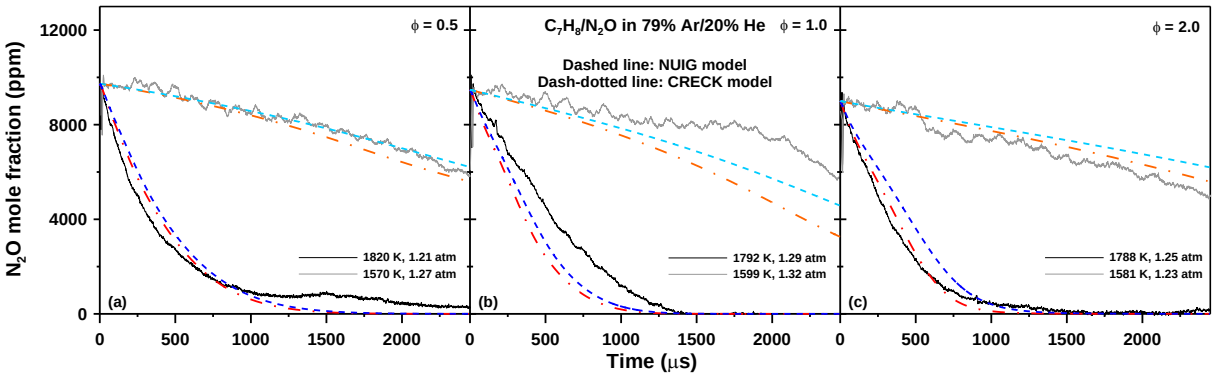

Figure 3: Evolution with time of the N_2O mole fraction during the oxidation of toluene by N_2O for mixtures diluted in 99% Ar and He and comparison with models from the literature. (a) $\phi = 0.5$, (b) $\phi = 1.0$, and (c) $\phi = 2.0$.

5 Conclusions

The time history of N_2O was followed by laser absorption spectroscopy during the combustion of toluene/N_2O mixtures for the first time. The data are useful for validating kinetics models for the development of spark ignition engines using a dual fuel setup with gasoline and ammonia. Results showed that the N_2O consumption varies greatly with the temperature but is weakly impacted by the equivalence ratio under the conditions investigated.

Models from the literature were generally capable of reproducing the data but room for improvement remains, especially for the stoichiometric and fuel-rich cases. A numerical analysis showed that the reactivity is initiated by the fuel thermal decomposition, leading to the formation of H and benzyl radicals. These H radicals will then react with toluene or N_2O to initiate the N_2O consumption by forming OH and nitrogen. This pathway is the preferred N_2O consumption pathway under our conditions, but a large contribution is also coming from the thermal decomposition of N_2O.

6 Acknowledgments

AB thanks Research Council of Finland (grant no. 346918) and Merenkulun säätiö for the financial support of this study. Computational resources provided by the Aalto Science-IT project are also acknowledged. The work at Texas A&M University was supported in part by the TEES Turbomachinery Laboratory.

References

[1] Mathieu O, Petersen EL. (2023). Carbon Free Fuels. ACS in Focus. American Chemical Society. (eISBN: 9780841299696).

[2] Valera-Medina A, Xiao H, Owen-Jones M, David WIF, Bowen PJ. (2018). Ammonia for power. Prog. Ener. Comb. Sci. 69: 63. Oppenheim AK. (1966). Novel Insight into the detonation process. Acta Astronaut. 11: 391.

[3] Mathieu O, Petersen EL. (2015). Experimental and modelling study on the high-temperature oxidation of Ammonia and related NOx chemistry. Combust Flame 162: 554.

[4] Mounaïm-Rousselle C, Brequigny, P. (2020). Ammonia as Fuel for Low-Carbon Spark-Ignition Engines of Tomorrow's Passenger Cars. Front. Mech. Eng. 6: 70.

[5] Guiberti TF, Pezzella G, Hayakawa A, Sarathy MS. (2023). Mini Review of Ammonia for Power and Propulsion: Advances and Perspectives. Energy&Fuels 37: 14411.

[6] Ravishankara AR, Daniel JS, Portmann RW. (2009). Nitrous Oxide (N_2O): The Dominant Ozone-Depleting Substance Emitted in the 21st Century. Science 326: 123.

[7] Vandebroek L, Van den Schoor F, Verplaetsen F, Berghmans J, Winter H, van't Oost E. (2005). Flammability limits and explosion characteristics of toluene–nitrous oxide mixtures. J. Haz. Mat. 120: 57.

[8] Kustova AL, Benavente Donaire PS, Koklina AE, Bogdan VI. (2014). Partial Oxidation of Toluene with Nitrous Oxide under Supercritical Conditions. Kinet. Catal. 55: 93.

[9] Zhou S, El-Sabor Mohamed, AA, Nagaraja SS, Wang P, Murakami Y, Liu J, Senecal PK, Curran HJ. (2024). An experimental and modeling study of hydrogen/n-decane blends. Combust. Flame 270: 113792.

[10] Bagheri G, Ranzi E, Pelucchi M, Parente A, Frassoldati A, Faravelli T. (2020). Comprehensive kinetic study of combustion technologies for low environmental impact: MILD and OXY-fuel combustion of methane. Combust. Flame 212: 142.

[11] Liang J, Zhao Z, Zhang, N, Li X, Cao Y, Li Y, Kong X, Wu Y, Dong S.(2024). Probing the effects of NO_2 and N_2O additions on the auto-ignition behaviors of gasoline at engine relevant conditions. Combust. Flame 259: 113188.

[12] Mathieu O, Mulvihill CR, Petersen EL. (2019). Assessment of modern detailed kinetics mechanisms to predict CO formation from methane combustion using shock-tube laser-absorption measurements. Fuel 236 1164.

[13] Rothman LS, Gordon IE, Barber RJ, Dothe H, Gamache RR, Goldman A, Perevalov VI, Tashkun SA, Tennyson J. (2010). HITEMP, the high-temperature molecular spectroscopic database, J. Quant. Spectrosc. Ra. 111: 2139.